

Full Paper

Synthesis of Dodecanol-Anchored Nano-sized Magnesium Imprinted Polymer and Its Application as an Efficient Ionophore in Mg²⁺-Selective PVC Membrane Electrode

Taher Alizadeh,* Maedeh Akhoundian, and Babak Hoseinnejad

Department of Analytical Chemistry, Faculty of Chemistry, University College of Science, University of Tehran, P.O. Box 14155-6455, Tehran, Iran

*Corresponding Author, Tel.: +98-21-61112788

E-Mail: talizadeh@ut.ac.ir

Received: 27 September 2021 / Received in revised form: 17 November 2021 /

Accepted: 20 November 2021 / Published online: 31 December 2021

Abstract- Magnesium imprinted polymeric (Mg-IP) nanoparticles were prepared by precipitation polymerization method in acetonitrile. Itaconic acid (ITA) and ethylene glycol dimethacrylate were employed as functional monomer/complexing agent and cross-linker, respectively. Fast Fourier-infrared spectroscopy was employed to investigate the interaction of ITA with Mg²⁺ ion. The obtained polymeric material was utilized as ionophore in order to fabricate the Mg²⁺-selective PVC-membrane electrode. The Mg-IP nanoparticles were covalently modified with alkyl chains, capping the surface carboxylic acid groups of the IPs and making them much hydrophobic. This strategy caused remarkably improvement in the electrode selectivity and durability. The optimized electrode showed response time of about 25 s and exhibited no memory effect. A dynamic linear range of 5×10^{-7} to 1×10^{-1} mol L⁻¹, Nernstian slope of $29.5 \pm (0.4)$ mV decade⁻¹ and detection limit of 2.3×10^{-7} mol L⁻¹ were attained for the electrode. The efficiency of the electrode was tested by the determination of Mg²⁺ amount in different bottled mineral water and drinking water samples.

Keywords- Magnesium; Imprinted polymer; Nano-sized; PVC membrane electrode; Alkyl chain

1. INTRODUCTION

Magnesium is a significant element in human body considering its various functions in biological systems. It is a co-factor for numerous enzymes involved in protein and DNA synthesis, production and storage of cellular energy, growth and reproduction of cells, stabilization of mitochondrial membranes and maintenance of cellular electrolyte composition [1-3]. Regarding the described biochemical activities, Mg^{2+} ions play a definitive role in control of neuronal activity, cardiac excitability, blood pressure muscular contraction and neuromuscular transmission [4].

A low level of Mg^{2+} has been noted in the patients that are suffering from migraine and cardiac illness. On the other hand, magnesium oversupply can cause coma and even death. Magnesium can be found in a number of dietary products such as meat, fish, seafood, dairy products, etc. It is also present in hard and mineral water in high quantities. Magnesium is utilized for making machine parts, moving at high speed and cathodic protection of other metals. It is also very useful in aerospace applications due to its lightweight associated with high strength [5].

Therefore, magnesium determination in industrial, biological, environmental as well as food samples is so essential [6]. Various analytical methods including atomic absorption spectroscopy [7,8], inductively coupled plasma-atomic emission spectroscopy [9], ion chromatography [10] and colorimetric method [11] have been employed to determine magnesium in different samples. However, the majority of these methods are time consuming and expensive and cannot be used for routine analysis in case of large number of samples.

Regarding the well-known advantages of the chemical sensors, compared to the instrumental methods, in the analytical applications they have been already considered for chemical analysis. Various kinds of chemical sensors, based on different sensing principals including Fluorescence [12], ion channel [13], voltammetry [14] and potentiometry [15], have been reported for Mg^{2+} determination. Recently, considerable numbers of different chemical sensors, designed for Mg^{2+} determination in biological samples, are surveyed and discussed within a review article [16].

Potentiometric ion-selective electrodes provide convenient, affordable, fast, and in-situ alternative for magnesium determination. So far, several Mg^{2+} selective electrodes have been reported in the literatures [17-26]. However, large number of these electrodes present narrow range of working concentration, long response time and suffer from other alkaline earth metal ions interfering, especially calcium [6]. Therefore, the development of new Mg^{2+} selective electrodes, possessing improved analytical characteristics, will be the beneficial research field. Imprinting in polymeric matrix is an effective methodology to synthesize the host materials, capable of recognition of target guest species. For this aim, functional monomers are allowed to surround the target molecule or ion. The monomers are subsequently copolymerized with a cross linker to form a material which can be used as the template recognition agent after

removal of the trapped species [27-32]. Imprinted polymers (IP) have been reported to act as ionophore in the potentiometric sensors designed for assessment of different kinds of ionic species [33-42].

In this procedure, we have utilized a commercially available functional monomer to synthesize Mg^{2+} -imprinted polymer (Mg-IP) and then its use for the fabrication of Mg^{2+} selective poly (vinyl chloride) (PVC) membrane electrode. The experimental results showed that itaconic acid (ITA)- Mg^{2+} complex, cross-linked with ethylene glycol dimethacrylate (EGDMA), results in a novel Mg^{2+} selective imprinted polymer nanoparticles which could act as an efficient Mg^{2+} ionophore in a PVC membrane electrode. Furthermore, we showed that surface modification of the imprinted polymeric particles by alkyl chains, could improve significantly the selectivity of the imprinted polymer-based electrode as well as other analytical characteristics of the electrode.

2. Experimental

2.1. Reagents and instruments

Divinylbenzene (DVB), ethylene glycol dimethacrylate (EGDMA), 2, 2-azobisisobutyronitrile (AIBN), sodium tetraphenyl borate (NaTPB) and high molecular mass poly (vinyl chloride) (PVC) were purchased from (Sigma-Aldrich, USA). Itaconic acid (ITA), di-nonyl phthalate (DNP), di-butylphthalate (DBP), tetrahydrofuran (THF), oleic acid (OA) was obtained from (Merck, Germany). All other chemicals were of analytical reagent grade and obtained from (Merck, Germany). Distilled water was used all over the experiments. Ag/AgCl (sat.) electrode was utilized as a reference electrode. Polyvinyl chloride (PVC) membrane electrode, impregnated with the synthesized imprinted polymer, was employed as indicator electrode. A corning ion analyzer 250 pH/mV meter was used for the measurement of potential response of the membrane electrode. LEO 1430VP scanning electron microscope (SEM) (Germany-England) with the accelerating voltage of 15 kV was employed to study the surface morphology of the imprinted polymer particles.

2.2. Synthesis of nano-sized Mg^{2+} -imprinted polymer

For preparation of Mg^{2+} -imprinted polymer, 0.5 mmol of Magnesium nitrate was transferred to a vessel, which contains 30 mL of ethanol and dissolved in it. Then, 1.5 mmol of itaconic acid was added and waited for 1 h to form the Mg^{2+} -ITA complex in the solution. Afterwards, 15 mmol of EGDMA as well as 0.05 g of AIBN was added to the mixture. Finally, purging of the resulting mixture with nitrogen gas for 15 min was carried out. The vessel was then sealed precisely and transferred to a water bath (60 °C), to start the polymerization reaction. This mixture was stirred continuously during the polymerization process while the polymerization reaction lasted 24 h. At the end of the polymerization, the obtained polymer powder was filtered and washed several times with water, hot ethanol and EDTA solution (pH=11, 1 mol L⁻¹) for the removal of the non-reacted

monomers as well as Mg^{2+} ion species from the polymer. The non-imprinted polymer (NIP) was also synthesized similar to the imprinted polymer, except that Mg^{2+} was not present during the process.

2.3. Modification of the polymeric particles with alkyl chains

In this step, for attaching the alkyl group to the surface of networked polymer particles, 0.5 g of the synthesized IIP (or NIP) was dispersed in toluene (30 mL). 10 g of dodecanol and 0.05 g of p-toluenesulfonic acid was then added to this container. The resulting mixture was refluxed for 24 h at 100 °C. To separate the solid from the liquid, the obtained sample was centrifuged and separated polymeric material was washed several times using toluene, methanol and water, respectively. Finally, it was dried at 60 °C.

2.4. Rebinding experiments

In order to evaluate the rebinding characteristic of Mg^{2+} ion to the imprinted polymer, the following procedure was carried out: 50 mg of polymer nano-particles were dispersed in 3.0 mL of the Mg^{2+} aqueous solution (0.01–2.0 mmol L⁻¹). This mixture was incubated while it was stirred continuously, at room temperature for 5 h. The sample tubes were then centrifuged and the supernatants were separated. Atomic absorption spectroscopy (AAS) method was then employed to analyze the aliquots.

Subtracting the free concentration of Mg^{2+} from the initial concentration, results in an amount of Mg^{2+} , extracted by the IIP (Q). This Data were processed due to the Scatchard equation (Eq. 1) to estimate the binding properties:

$$\frac{Q}{C_e} = \frac{Q_{\max} - Q}{K_d} \quad (1)$$

where C_e ($\mu\text{mol mL}^{-1}$) is the free concentration of Mg^{2+} at equilibrium, Q_{\max} ($\mu\text{mol g}^{-1}$) is the apparent maximum number of binding sites and K_d (mol L^{-1}) is the dissociation constant.

2.5. Fabrication of the sensor

For the fabrication of PVC membrane sensor, the Mg^{2+} -imprinted or non-imprinted polymer nanoparticles were dispersed in 2.5 mL of tetrahydrofuran (THF). Then, DBP, NaTPB and PVC powder was added. This mixture was then sonicated for 10 min in order to entirely dissolve or disperse the solution content in THF. The obtained solution was subsequently transferred into the Teflon mold (20 mm diameter) and THF was taken off by vaporization at room temperature. The thickness of the prepared membrane was estimated to be about 0.5 mm. A small part of the resulting membrane (5 mm diameter) was cut and mounted

on a Pyrex tube (i.e. 3 mm, o.d. 6 mm) via PVC glue. This tube was filled finally with an internal filling solution (10^{-1} mol L⁻¹ of Mg²⁺).

2.6. Analytical procedure

The IIP-based electrode was conditioned in 0.1 mol L⁻¹ of Mg²⁺ solution for 24 h. The electromotive force (EMF) of the following electrochemical cell was quantified as the response of the membrane electrode:

(Ag-AgCl (internal reference electrode) | internal solution (1.0×10^{-1} mol L⁻¹ Mg²⁺) | PVC-IIP membrane | sample solution | Ag-AgCl (external reference electrode))

In order to measurement the potential signals, the reference electrodes (external and internal reference electrodes) were connected to a corning ion analyzer 250/pH mV meter. The potential responses of the sample solutions with different amounts of Mg²⁺ were recorded and plotted as a function of Mg²⁺ concentration.

2.7. Mg²⁺ sensor application for real samples

In real samples, the analysis of magnesium ion content was performed using the standard addition technique. The pH of the samples, aimed to be analyzed, was adjusted to 7. Then, the samples were spiked with increments of known magnesium solution (0.10 mol L⁻¹). The following equation (equation 2) was utilized for potentiometric analysis of Mg²⁺ ions via the standard addition method:

$$C_x = \frac{C_s \times V_s}{(V_s + V_x) \times 10^{\frac{\Delta E}{S}} - V_x} \quad (2)$$

where, ΔE is the potential difference formed as a result of standard addition. C_x and C_s stand for concentrations of Mg²⁺ ion in water and standard solution, respectively. V_x and V_s are the corresponding volumes and S is the slope of the calibration graph, plotted as the sensor response versus magnesium ion concentration. Drinking and mineral water samples were tested without any pretreatment. Plasma samples, obtained from Tehran University Hospital (Tehran, Iran), were deproteinized using perchloric acid solution (2 mol L⁻¹), before performing the determination method. However, the sample solution pH was adjusted to 7, before potentiometric measurement of Mg²⁺.

For the analysis of dried milk samples, an accurately weighed quantity of the sample was transferred to a silica crucible. Then, several drops of concentrated nitric acid were added to the powder, followed by heating of the crucible in a furnace at 400 °C for 1 h. The dish was removed and after cooling, its ash content was moistened with a few drops of concentrated sulfuric acid. Again, the crucible was placed on the heater, until the fumes of sulfuric acid disappeared. Crucible containing the ash was then heated in furnace up to 600 °C (1 h). Finally,

concentrated HCl (3 ml), was added to the resulting material and the volume was made to 20 ml by distilled water in a measuring flask. The obtained solution was used directly for its magnesium content analysis by both AAS and the prepared sensor, after adjusting the pH of the samples to 7.

3. RESULT AND DISCUSSION

3.1. Synthesis of the imprinted polymer

As a well-known principal, in the imprinted binding sites, functional monomers are responsible for the binding interactions. The basis for the recognition properties of MIP is provided by the nature and extent of the molecular interactions, present in the pre-polymerization phase. A key step in the polymer synthesis is the formation of the pre-complex between the template and functional monomer(s). It is obvious that stronger interactions between the template and monomers leads to more stable host-guest complex, prior to polymerization, resulting in more efficient imprinting [43].

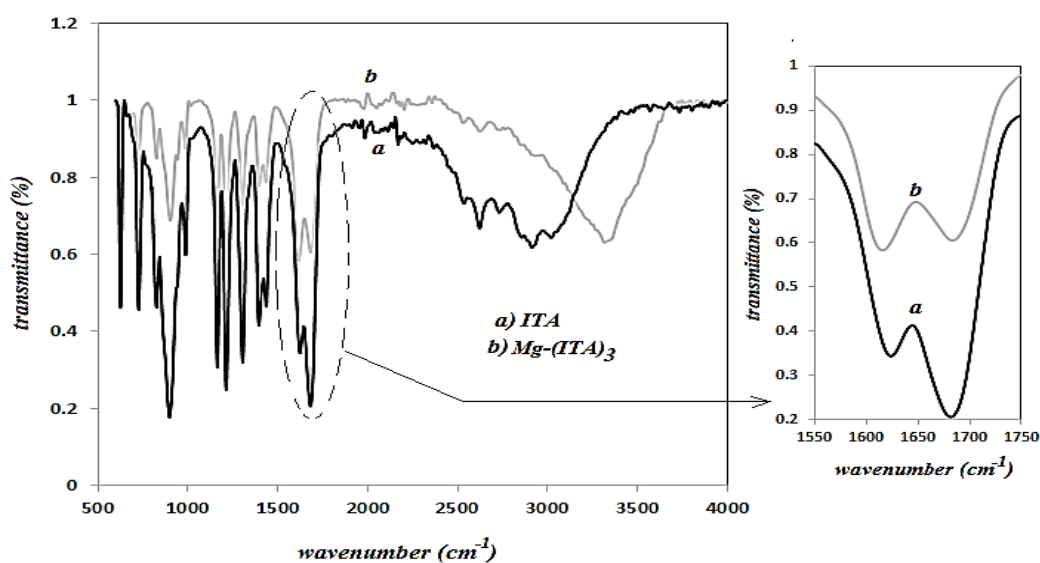


Fig. 1. FT-IR spectra of ITA (a) and ITA-Mg²⁺ complex (b)

The interaction of Mg²⁺ ion with the functional monomer of ITA was investigated using fast fourier-infrared spectroscopy (FT-IR) technique. The results obtained are shown in Fig. 1. In FT-IR spectrum of ITA two characteristic absorption bands in 1683 cm⁻¹ and 1623 cm⁻¹ can be assigned to the C=O and C=C groups, respectively. The other characteristic IR peak of ITA acid is the broad band at 2960 cm⁻¹, attributed to OH groups involved in hydrogen bonding. As can be seen, the interaction of Mg²⁺ ion with ITA and forming the complex between them, has led to reduce the intensity of C=O related band. This decrease is due to the contribution of these carbonyl groups in the complexation with metal ion. The rigid structure of the Mg²⁺-ITA

complex reduces vibration of the atoms in the complex structure and therefore leads to the lower peak intensities. Most importantly, it can be seen that the complexation reaction affects the band of 1683 cm^{-1} more intensive than that of 1623 cm^{-1} , leading thus to decrease the peaks height ratio (the ratio of the first peak to the second peak) from 1.5 to about 1. These observations suggest that the oxygen atoms of both carbonyl groups of ITA participate in the interaction with Mg^{2+} and making the related complex compound. On the other hand, very significant shift is seen in the FT-IR band related to stretching vibration of OH, as a result of the complexation reaction with Mg^{2+} . This is because of librating of the OH groups from hydrogen bonding with C=O groups, due to the actively involvement of C=O groups in the complexation with metal ion.

Basically, FT-IR spectrum of ITA represents the IR adsorption information of the ITA within a molecular network. This means that the molecule of interest is involved in interactions with other the same molecules. Regarding the chemical structure of ITA, it seems that every ITA molecule interacts strongly with the other ITA molecules via strong hydrogen bonding. This means that both carboxylic acid groups of each ITA molecule are involved effectively in hydrogen bonding, leading to considerable decrease in the C=O stretching frequency.

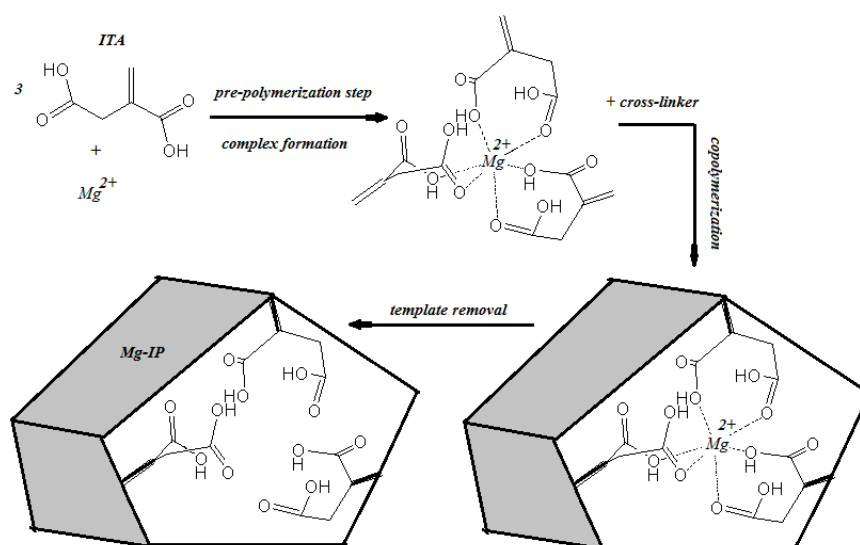


Fig. 2. Schematic representation of Mg^{2+} -imprinted polymer synthesis procedure

This is also results in broadening of the O-H vibration related adsorption band and its shifting to lower wavenumber in the FT-IR spectrum of ITA., interaction of Mg^{2+} with ITA molecules can destroy the previously describe ITA-ITA acid liberating the C=O and O-H functionalities from the hydrogen bonding. However, the C=O groups released from the hydrogen bonding are again involved in interaction with Mg^{2+} as a result of complexation reaction. Since, there is no significant difference in the position of C=O band in the FT-IR spectra of ITA and Mg^{2+} -ITA, one can predict that the interaction power of Mg^{2+} with C=O

group of ITA is not considerably higher than the hydrogen bonding power within two ITA molecules interacted with each other. However, significant shift of OH band to higher wavenumber value as a result of ITA and Mg^{2+} reaction confirms the Mg^{2+} -ITA complexation reaction. Fig. 2 represents schematic representation of Mg^{2+} -imprinted polymer preparation method, utilized in this study. Based on the depicted scheme, both carboxylic groups of ITA acids, surrounding the metal ion, can interact with it and participate in ion recognition.

3.2. Capping of surface functional groups of the IIP by hydrophobic alkyl chains

It was previously proven that carboxylic acid functional groups, originated from the functional groups, used for the imprinted polymer creation, can be situated on the imprinted polymer surface and act as a source for the non-specific interaction. This gives rise to the appearance of non-selective behavior of the IP-based membrane electrode [36]. Therefore, in this study, we decided to cap the free carboxylic acid groups of the IP particles, not involved completely in the imprinting process. For this aim, alkyl chains, provided by dodecanol, were anchored on the IP particles via esterification reaction, as illustrated schematically in Fig. 3.

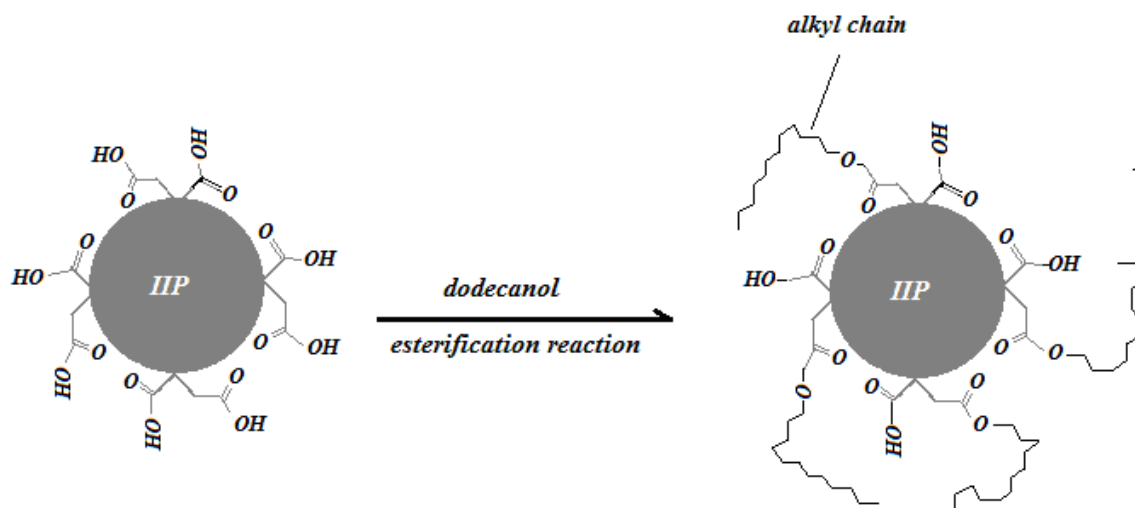


Fig. 3. schematic representation of the modification of the IP nanoparticles by anchoring of linear alkyl chains on their surfaces via esterification reaction

Fig. 4 exhibits the FT-IR spectra of both unmodified and modified Mg -imprinted polymers. The presence of new peak at wavenumber of 2880 cm^{-1} in the modified IIP, which is absent in the unmodified IIP spectrum, can be attributed to alkyl chains, anchored to the IIP particles. It must be mentioned that the small band at about 2600 cm^{-1} in the FT-IR spectrum of the unmodified IIP is assigned to CO_2 impurity in the sample.

Scanning electron microscopy images of the modified IIP, unmodified IIP and its corresponding NIP are represented in Fig. 5. According to the size distribution diagram,

illustrated in the inset of the figure, most of IIP particles have diameters below 100 nm. Furthermore, one can easily see that there is no remarkable difference between the modified IIP and unmodified IIP regarding the morphology of the polymeric particles shown in the images. It is also obvious that there is not any significant difference between the IIP and NIP materials regarding the particles morphology.

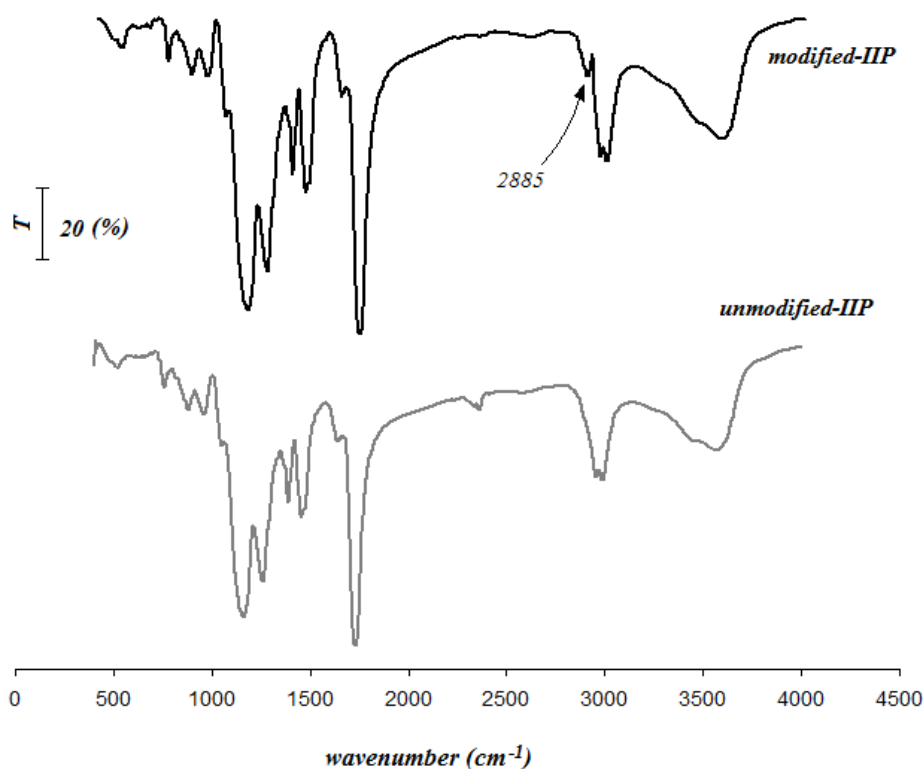


Fig. 4. FT-IR spectra of the Mg²⁺-imprinted polymers before and after modification by alkyl chains

3.3 Investigation of Mg²⁺ rebinding property of the IIP nanoparticles

In order to investigate the binding properties of the modified- and unmodified-IIP nanoparticles, they were examined by a rebinding experiment within Mg²⁺ concentration, ranged from 0.01 to 2.0 mmol L⁻¹. The same experiment was performed using the corresponding NIP nanoparticles. Binding data were processed afterwards with Scatchard plot (Eq.1). The obtained results are represented in Fig. 6. It can be seen that in cases of both IIPs the Scatchard plots represent two different linear curves, assigned to two kinds of the recognition sites. This demonstrates that the binding sites of the imprinted polymers are heterogeneous with respect to Mg²⁺ ion, which can be classified into two distinct groups including the high-affinity and the low-affinity binding sites. The linear regression equations for the two lines of the Scatchard plot for the modified-IIP are $Q/C_e = 17076 - 1833.4Q$ ($r=0.996$) and $Q/C_e = 271.03 - 15.82Q$ ($r=0.882$). Using the slope and intercept of Scatchard plot, the

equilibrium dissociation constant (K_d) and the apparent maximum number (Q_{max}) were calculated to be $5.45 \times 10^{-4} \text{ mol L}^{-1}$ and $9.31 \mu\text{mol g}^{-1}$ for the high-affinity binding sites, and $6.3 \times 10^{-2} \text{ mol L}^{-1}$ and $17.15 \mu\text{mol g}^{-1}$ for the low-affinity ones.

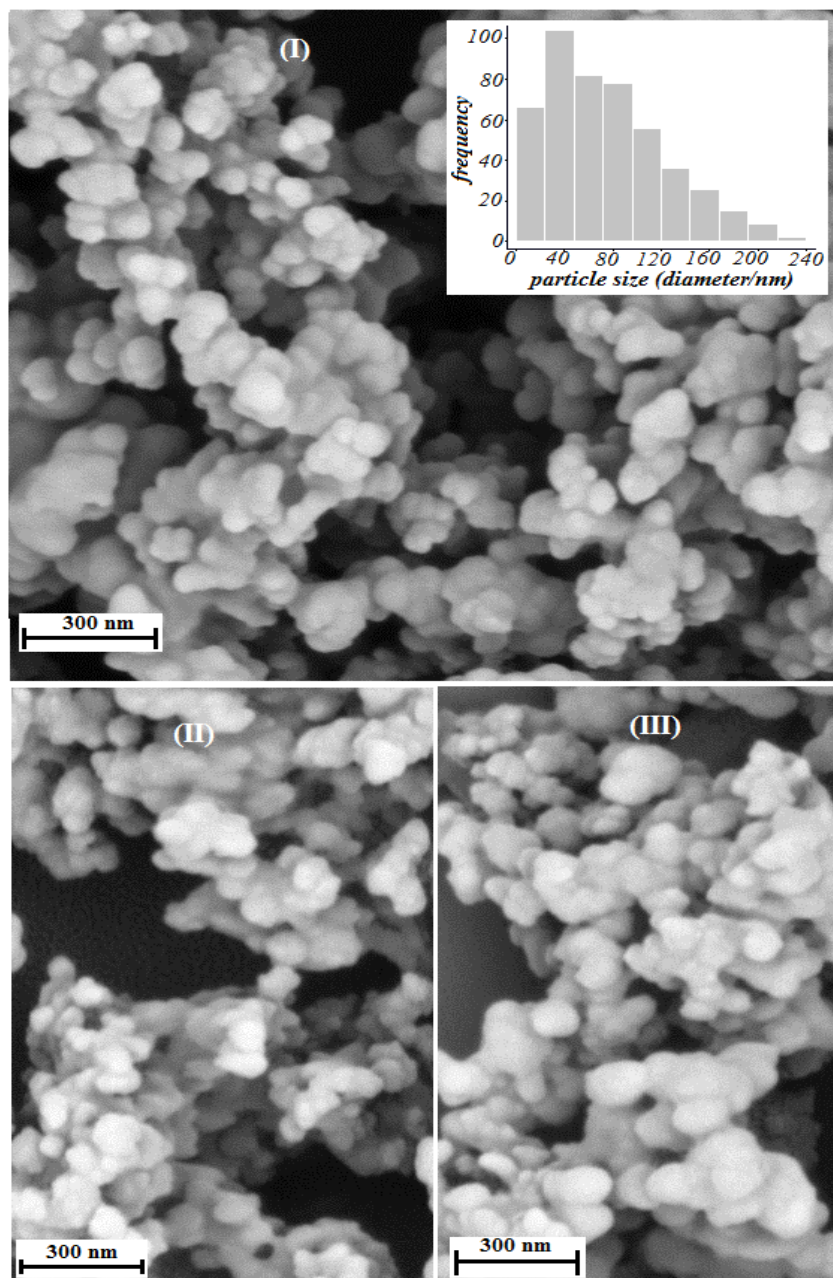


Fig. 5. scanning electron microscopy image of modified-imprinted polymer (I), modified unimprinted polymer (II) and non-imprinted polymer (III)

The linear regression equations for the two lines of the Scatchard plot of the unmodified-IIP are $Q/C_e = 14760 - 1462.1Q$ ($r = 0.938$) and $Q/C_e = 1529.0 - 74.36Q$ ($r = 0.946$). Based on these equations the K_d and the Q_{max} of the unmodified-IIP were calculated to be $6.8 \times 10^{-4} \text{ mol L}^{-1}$ and $10.1 \mu\text{mol g}^{-1}$ for the high-affinity binding sites, and $1.3 \times 10^{-2} \text{ mol L}^{-1}$ and $20.56 \mu\text{mol g}^{-1}$ for

the low-affinity ones. Comparing of the K_d and the Q_{max} values of both IIPs either in the case of low affinity sites or high affinity sites indicates that modification of the IIP surface has only slight effect on the K_d and the Q_{max} of the polymer in high affinity sites; however, the modification results in a significant (about 5 times) increase in the K_d value of the low affinity sites.

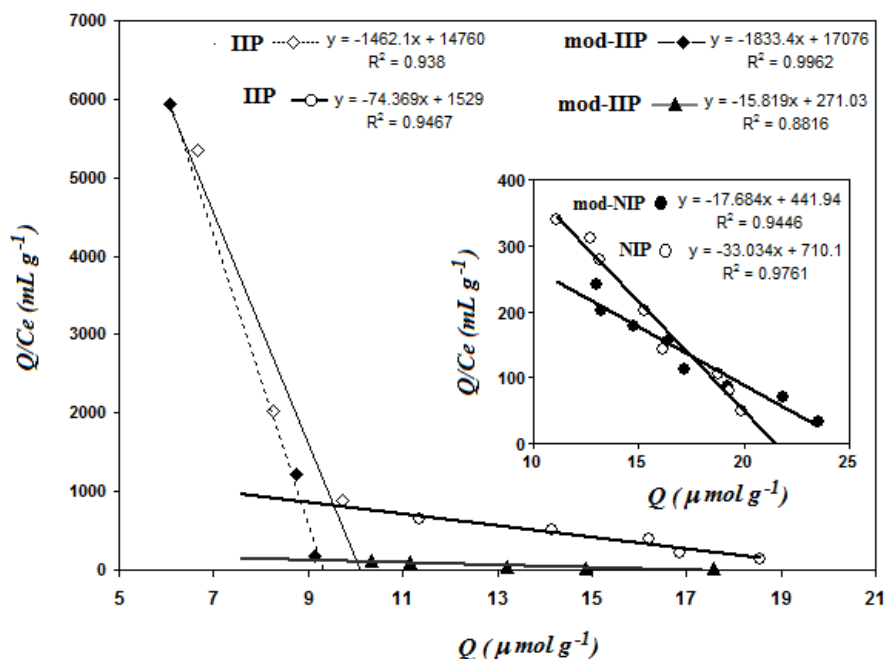


Fig. 6. Scatchard plot obtained as a result of evaluation of the data of Mg^{2+} ion rebinding to the modified and unmodified-imprinted polymer; Scatchard plot obtained for the modified- and unmodified-NIP (inset)

This means that surface functional groups of the IIP are mainly capped by the alkyl chains and thus the interaction of Mg^{2+} ions with the surface sites are weakened considerably. Furthermore, the results show that the functional groups situated in the main recognition sites of the IIP (selective cavities) have not meaningfully influenced by the modification reaction. Regarding the inset of Fig. 6, it can be seen that the Scatchard plots of both NIPs (modified- and unmodified-NIPs) represent a linear curve. This indicates that the binding sites in both modified- and unmodified-NIP are only low-affinity binding sites. The linear regression equations for the Scatchard plot of the modified- and unmodified-NIP are $Q/C_e = 441.6 - 17.68Q$ ($r = 0.944$) and $Q/C_e = 710.1 - 33.03Q$ ($r = 0.976$), respectively. From the slope and intercept of Scatchard plot, the K_d and Q_{max} of the modified-NIPs were calculated to be 5.65×10^{-2} mol L⁻¹ and 24.97 μmol g⁻¹, respectively. Furthermore, for the unmodified-NIP the K_d and Q_{max} values were estimated to be 7.5×10^{-3} mol L⁻¹ and 5.33 μmol g⁻¹ for the low-affinity ones. Again, it is clear that the modification gives rise to considerable decrease in the affinity of the NIP material to Mg^{2+} because of lost in surface functional groups as a result of modification.

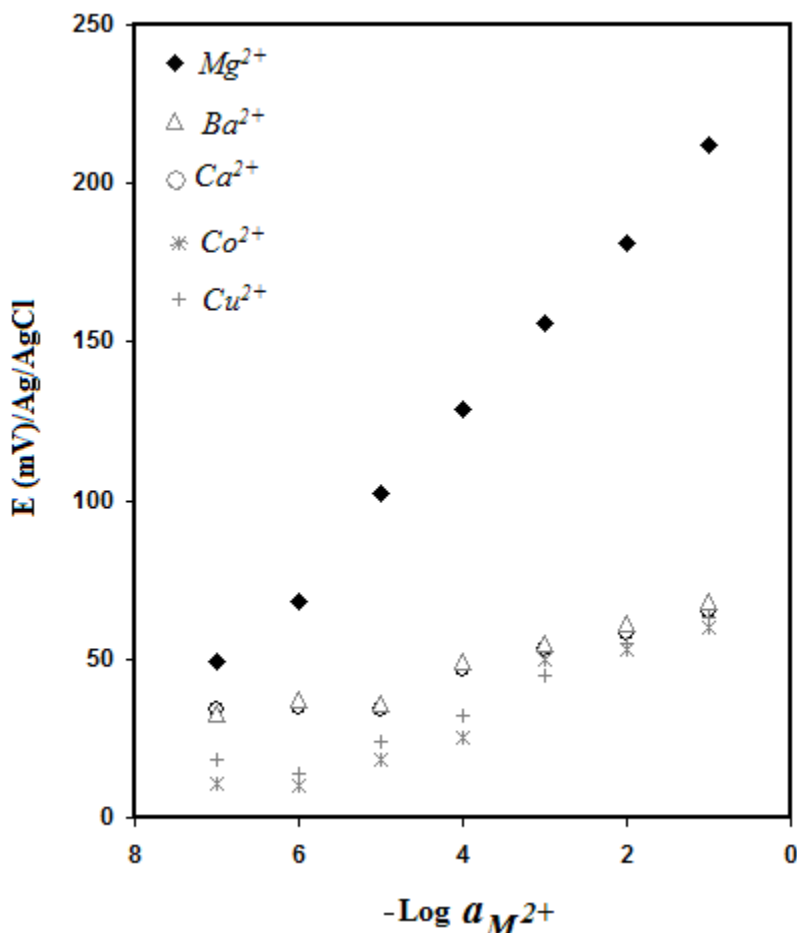


Fig. 7. Potentiometric response of the alkyl chain-modified IIP nanoparticles-based membrane electrode to target ion of Mg^{2+} and some other foreign cations

3.4. Application of surface modified magnesium-imprinted polymer as Mg^{2+} ionophore

After the capping of the surface located active functional groups of the IIP particles, they were incorporated with PVC membrane electrode to prepare modified-IP-based Mg^{2+} selective electrode. The potentiometric responses of the electrode obtained were examined in the presence of different concentrations of Mg^{2+} as well as various concentrations of some potentially interfering cationic agents. The obtained results are illustrated in Fig. 7. It is evident that the electrode responds to Mg^{2+} in a near-Nernstian manner ($27.5 \text{ mV decade}^{-1}$, between 1×10^{-7} - $1 \times 10^{-1} \text{ M}$). More interestingly, it can be seen that the electrode exhibits significantly lower sensitivity to other ions tested (compared to its sensitivity to target ion of Mg^{2+}).

3.5. Optimization of the membrane composition

Sensor behavior is affected by the membrane composition that was investigated in order to establish the appropriate composition for the electrode [44-51]. The obtained results are summarized in Table 1.

Table 1. optimization of the composition of the modified-IIP-based membrane electrode

No.	PVC%	Plasticizer %			IIP%	Additive%		Slope mV/decade	Linear range (M)	R ²
		DNP	NPOE	DBP		Oleic	NaTPB			
1	24	68	-	-	5	6	-	11.4	1×10 ⁻⁴ -1×10 ⁻¹	0.92
2	24	68	-	-	5	-	6	18.8	1×10 ⁻⁵ -1×10 ⁻¹	0.95
3	24	-	68	-	5	-	6	19.3	1×10 ⁻⁴ -1×10 ⁻¹	0.98
4	24	-	-	68	5	-	6	22.4	1×10 ⁻⁵ - 1×10 ⁻¹	0.94
5	21	-	-	70	5	-	4	24.2	1×10 ⁻⁴ - 1×10 ⁻¹	0.96
6	25	-	-	68	3	-	4	14.6	1×10 ⁻⁵ - 1×10 ⁻¹	0.94
7	13	-	-	74	7	-	6	17.6	1×10 ⁻⁵ - 1×10 ⁻¹	0.97
8	21	-	-	65	11	-	3	24.8	1×10 ⁻⁶ -1×10 ⁻¹	0.98
9	21	-	-	67	10	-	2	24.5	1×10 ⁻⁵ - 1×10 ⁻¹	0.98
10	21	-	-	61	10	-	8	18.6	1×10 ⁻⁵ - 1×10 ⁻¹	0.99
11	20	-	-	68	7	-	5	29.9	1×10⁻⁶- 1×10⁻¹	0.99

As it is clear, the presence and also the kind of the ionic additive has crucial effect on linear range of the membrane electrodes as well as the calibration curve's slopes. Introducing oleic acid, although, improves slightly the curve slope, but the improvement is not satisfactory. However, changing of oleic acid to NaTPB improves noticeably the calibration curve slope from 11.4 to 18.8 mV decade⁻¹, which means that the sensor response approaches to Nernstian manner. Moreover, using NaTPB has led to the much more dynamic detection range, compared to the oleic acid-based membrane. On the other hand, it is indicated that, there is no favorable effect on the electrode performance by changing of membrane plasticizer from di-nonyl phthalate (DNP) to nitrophenyloctyl ether (NPOE). However, NPOE replacement with di-butyl phthalate (DBP) improves the calibration curve's slope significantly. The increasing of the IIP seems to improve the sensor sensitivity (increasing the calibration curve's slope). However, other examined membranes show that the correlation between the quantities of different ingredients of the membrane electrodes and their potentiometric characteristics is not easy task. This suggests that the synergistic effects exist among the quantities of the various membrane components. However, as shown in the Table 1, the membrane "11" is the best membrane due to potentiometric response slope as well as the detection range. Therefore, the membrane composed of PVC (20.0%), DBP (68.0%), IIP (7.0%) and NaTPB (5.0%) was chosen as the best membrane composition for the final sensor fabrication.

3.6. Response time and memory effect

The dynamic response time of the optimized sensor is illustrated in Fig. 8. According to this results, the response time of the sensor is approximately 25 s. Fig. 8 (inset) shows the response (potential–time) behavior of the electrode, against changing of Mg^{2+} concentration from 1.0×10^{-5} to 1.0×10^{-4} mol L⁻¹ and then from 1.0×10^{-4} to 1.0×10^{-3} mol L⁻¹ (via immediate injection of μ L amount of a concentrated solution; the raising parts of the curve) and then the reduction of Mg^{2+} concentration from 1.0×10^{-3} to 1.0×10^{-5} mol L⁻¹ by appropriate dilution of the solution (the descending part of the curve). This experiment was performed to test the hysteric effect of the developed sensor. It is obvious that the potentiometric response of the IIP-based electrodes was reversible and no memory problem was found for the sensor. The described curve indicates that recovery time of the electrode is longer than its response time (about 40 s). The considerably short response and recovery times of the developed sensor can be due to the nano-sized structure of the IIP material which leads to fast Mg^{2+} -rebinding kinetic because of the presence of the recognition sites of the IIP on its surface.

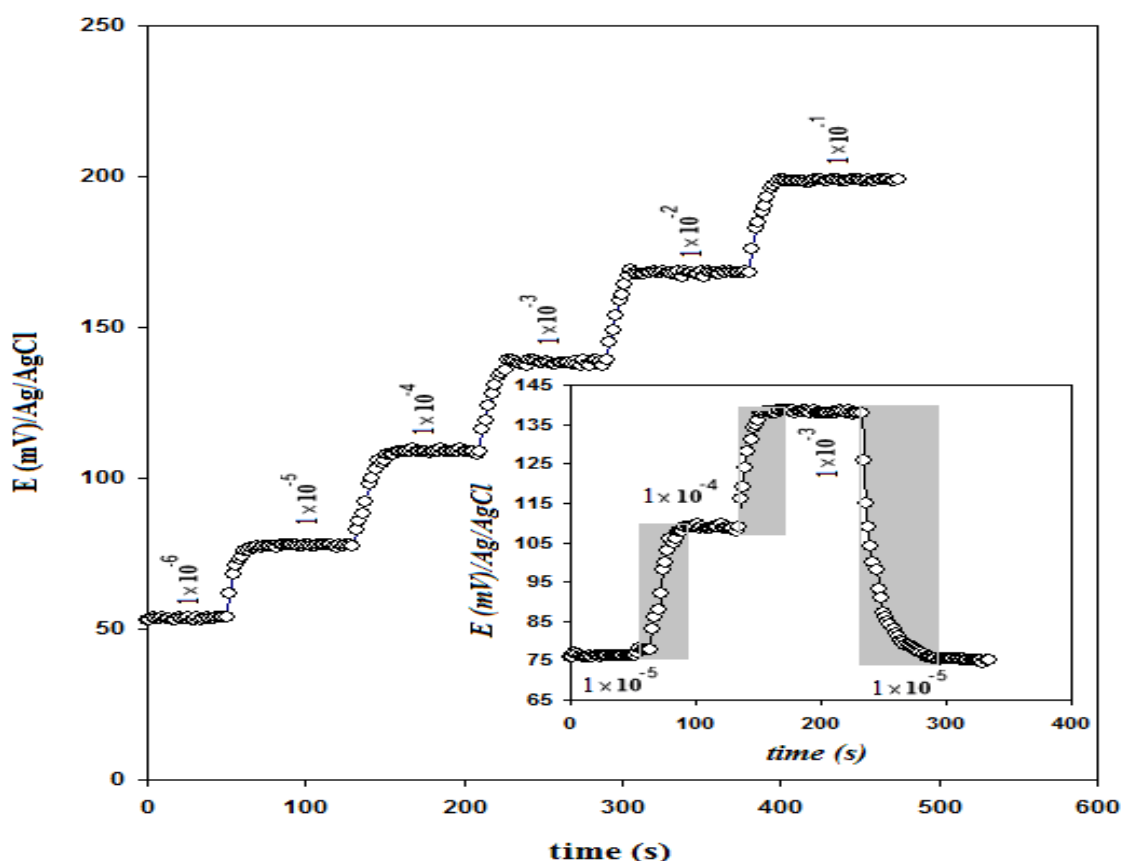


Fig. 8. dynamic response time curve of the imprinted polymer-based Mg^{2+} selective electrode; evaluation of recovery time and memory effect of the sensor (inset)

3.7. The effect of pH on optimized electrode performance

The effect of Mg^{2+} solution pH on the responses of the Mg^{2+} selective membrane electrode was examined by varying of the solution pH (in the range of 1.0–12.0) and recording the electrode potential response to 1×10^{-4} M of Mg^{2+} at each tested pH. The obtained results are shown in Fig. 9. According to the described results, the potential response of the electrode stays constant on a relatively large pH range (4.0–8.0). The electrode response deviates significantly from the constant value with increasing the pH above 8.0 or decreasing below 4.0. The loss of the electrode response in alkaline pH values could be due to the swelling of the IP nanoparticles within the PVC membrane, which is arisen from deprotonation of carboxylic acid groups in recognition sites of the imprinted polymers. As it is mentioned, when the pH of the solution is changed from 4 to lower values, the electrode response to Mg^{2+} deviates from the ideal condition. It comes to mind that the carboxylate groups, created as a result of deprotonation of the ITA carboxylic acid groups in the higher pH values, interact much effectively with Mg^{2+} ions, compared to carboxylic acid functional groups.

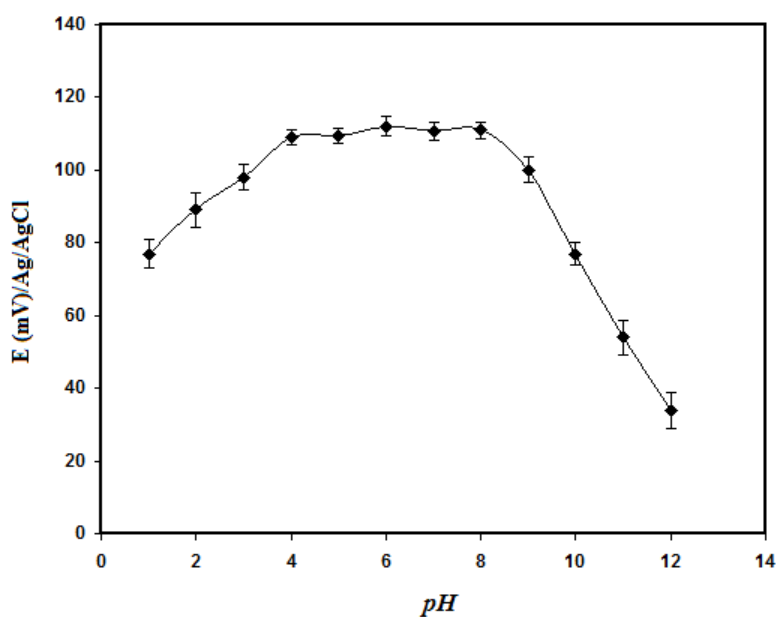


Fig. 9. the effect of solution pH on the sensing performance of the magnesium ion selective electrode

3.8. Analytical characteristic of the optimized sensor

The potentiometric selectivity coefficients of the electrode, prepared by the modified IP, were measured by the so-called fixed interference method (FIM). The resulting values were compared with those obtained for that fabricated with unmodified IIP nanoparticles. These results are illustrated in Fig. 10. It can be seen that the modification of the IIP particles results in a significant selectivity improvement for the related membrane electrode. The carboxylic acid functional groups situated on the IIP surface, can contribute in the non-specific adsorption

characteristic of the IIP and decreasing the selectivity of the unmodified IIP-based membrane electrode. As a result of hydrophobic alkyl chains anchoring to the IIP surface, a noticeable portion of the carboxylic acid groups, placed on the IIP surface, are blocked and increase the selectivity of the modified IIP-based sensor.

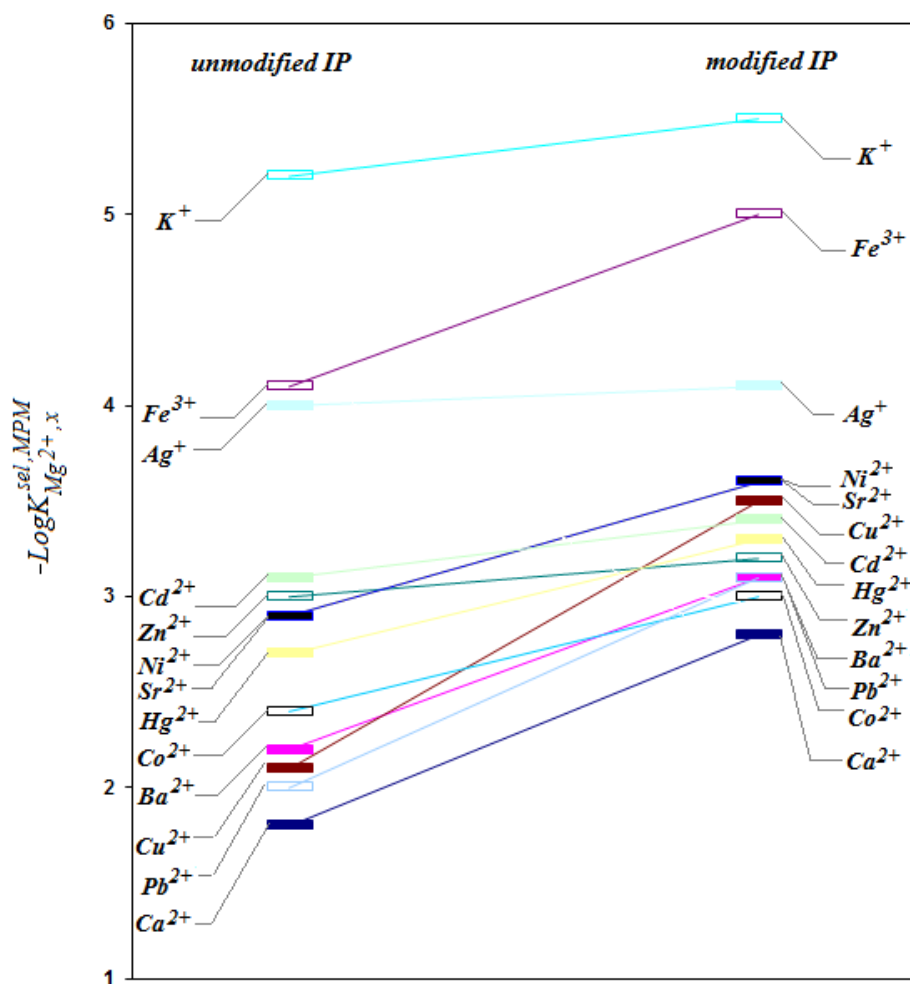


Fig. 10. Comparison of the selectivity coefficients of the IP-based membrane electrodes towards various kinds of ions before and after modification of the imprinted polymer

The modified-IIP membrane electrode as well as the blank electrode (the PVC membrane electrode containing modified-NIP in place of modified-IIP particles) was contacted to different concentrations of Mg^{2+} and the recorded potential responses were utilized to make the calibration curves. The obtained curves are depicted in Fig. 11 (I). Each potential response in the curves is the average of triplicate measurements of Mg^{2+} concentration. As it is clear, the presence of modified-IIP nanoparticles in the membrane electrode leads to a linear response (5×10^{-7} to 1×10^{-1} mol L⁻¹); whereas, there was no reasonable relationship between the potential response of the modified-NIP membrane and Mg^{2+} concentration. The slope of the calibration

curve, obtained for the modified IIP-based electrode, is about $29.5 (\pm 0.5 \text{ mV decade}^{-1})$ which can be considered as the Nernstian slope, assuming Mg^{2+} species responsible for the potential responses. The LOD of the sensor was $2.3 \times 10^{-7} \text{ mol L}^{-1}$, calculated based on the IUPAC definition.

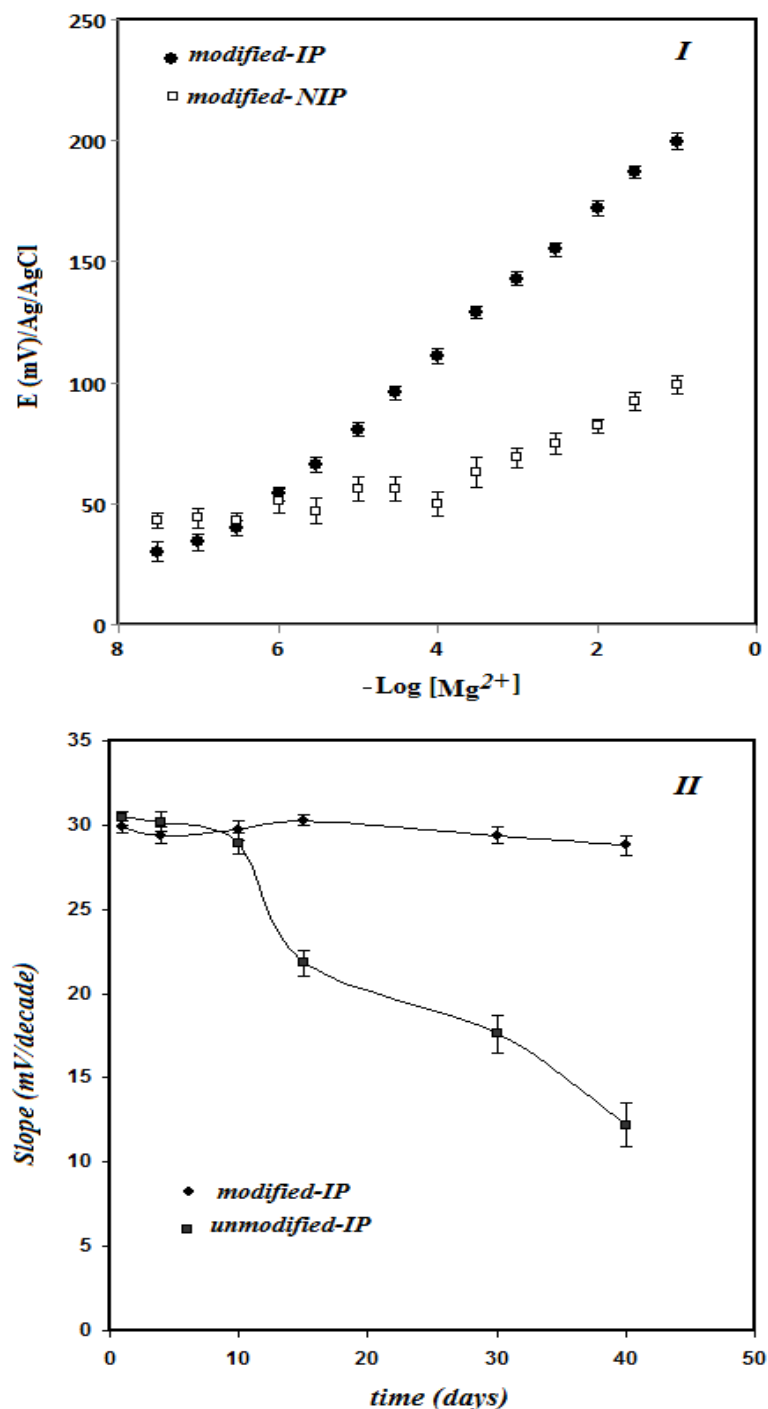


Fig. 11. Calibration curves of PVC membrane electrodes, prepared using modified nano-IP and nano-NIP particles as Mg^{2+} ionophores (I); comparison of the durability of the modified-IP and unmodified-IP based membrane electrodes (II)

In order to examine the durability of the membrane electrode, containing the modified IIP nanoparticles, the slope of the calibration curve of the electrode was recorded in different periods. It must be mentioned that the electrode was remained in buffer solution between different tests. The same experiment was also carried out by the membrane electrode fabricated by the unmodified IIP, in order to evaluate the modification effect on the electrode durability. Fig. 11(II) illustrates the the plot of calibration curve slope for each described electrode versus time. It is obvious that after about 40 days immersion of the modified-IIP based membrane electrode in the buffer solution no significant alteration is occurred in the response of the electrode to Mg^{2+} . However, according to the related plot, the response of the unmodified-IIP based membrane electrode starts to deviate considerably from Nernstian slope, after about 10 days. These results indicate that the modification of the IIP nanoparticles' surface with alkyl chains, is an effective way for the improvement of the life time for the related membrane electrode.

Table 2. The results of the application of the modified-IIP-based Mg^{2+} -selective electrode and reference AAS method to magnesium ion content analysis in different samples (n=3)

Sample	Mg^{2+} (ppm)		Critical value	Bias value
	Developed sensor	AAS method		
Tap water	25.6±1.3	24.7±1.5	2.1	0.9
Drinking water				
Aquafina	13.6± 0.6	12.8±0.5	0.8	0.8
Dasani	21.9± 1.1	22.3±0.9	1.5	0.4
Mineral water				
Damavad	11.4± 0.5	11.9±0.6	0.8	0.5
Vata	2.8±0.3	2.5±0.2	0.4	0.3
Dried milk				
Nan	0.51±0.04 ^a	0.48±0.03 ^a	0.05	0.03
Ladymil	2.14±0.15 ^a	2.21±0.11 ^a	0.2	0.07
Biological fluid^b				
Plasma 1	11.5±0.7	11.2± 0.5	0.8	0.3
Plasma 2	10.3±0.8	10.8±0.6	1.0	0.5

^a mg g⁻¹

^b ionized Mg^{2+} or free Mg^{2+}

$$\text{critical value} = \pm t.s \sqrt{\frac{N_1 + N_2}{N_2 \times N_2}}$$

In order to assess the applicability of the developed imprinted polymer-based ion selective electrode for real samples, the optimized electrode was used to measure Mg^{2+} content of different water samples. The samples, tested with the developed sensor, were also analyzed by AAS, as the reference method. The obtained results are illustrated in Table 2. Statistical analysis (the paired t-test, confidence level of 95%) suggested no significance differences between the Mg^{2+} concentrations, obtained by the developed electrode and those proposed by the reference method.

4. CONCLUSION

A novel nano-sized Mg^{2+} imprinted polymer was synthesized utilizing itaconic acid as complexing functional monomer, being as a cheap and commercially available monomer. FT-IR was used for the investigation of complex formation between ITA and Mg^{2+} in the pre-polymerization step. The recognition sites distribution of the IIP and their relative affinities to target ion of Mg^{2+} were evaluated by rebinding experiment and the Scatchard equation. The synthesized polymeric nanoparticles were used successfully as Mg^{2+} ionophore in the fabrication of a PVC-membrane electrode, capable of selectively determine Mg^{2+} ion. It was shown that capping of the IIP nanoparticles surface with the alkyl chains made them to be better Mg^{2+} ionophore in the fabrication of the Mg -selective membrane electrode. The electrode fabricated with the alkyl chain anchored-IIP, showed higher Mg^{2+} selectivity and longer life time limit, compared to the membrane electrode loaded with unmodified IIP as the Mg^{2+} ionophore.

REFERENCES

- [1] W. E. C. Wacker, *Magnesium and Man*, Cambridge, Harvard University Press (1980).
- [2] M. F. Ryan, *Ann Clin Biochem.* 28 (1991) 19.
- [3] M. E. Shils, *Ann. Rev. Nutrition* 8 (1988) 429.
- [4] B. T. Altura, T. L. Shirey, C. C. Young, K. Dellorfanio, J. Hiti, R. Welsh, Q. Yeh, R. L. Barbour, and B. M. Altura, *Scand. J. Clin. Lab. Invest.* 54 (1994) 21.
- [5] V. K. Gupta, S. Chandra, R. Mangla, *Sens. Actuators B* 86 (2002) 335.
- [6] P. Kumar, and Y. B. Shim, *J. Electroanal. Chem.* 661 (2011) 25.
- [7] A. Abarc, E. Canfran, I. Sierr, and M. L. Marin, *J. Pharm. Biomed. Anal.* 25 (2001) 941.
- [8] T. R. Williams, B. Wilkinson, G. A. Wadsworth, D. H. Barter, and W. J. Beer, *J. Sci. Food Agr.* 17 (1966) 344.
- [9] G. A. Meyer, J. S. Roeck, and T. Johnson, *Spectrochim. Acta B* 40 (1985) 237.
- [10] D. L. Smith, and J. S. Fritz, *Anal. Chim. Acta* 204 (1988) 87.
- [11] A. E. Harvey, J. M. Komarmy, and G. M. Wyatt, *Anal. Chem.* 25 (1953) 498.
- [12] F. Farruggia, S. Iotti, L. Prodi, N. Zaccheroni, M. Montaltu, P. B. Savage, G. G. Trapani, and F. I. Wolf, *J. Fluoresc.* 19 (2009) 11.

- [13] Y. Umezewa, and H. Aoki, *Anal. Chem.* 76 (2004) 320A.
- [14] J. Li, G. Zou, X. Hu, and X. Zhang, *J. Electroanal. Chem.* 625 (2009) 88.
- [15] J. Q. Y. Zhu, and Y. Zhang, *Anal. Chem.* 82 (2010) 436.
- [16] M. Algarra, C. M. Jimenez-Herrera, and J. C. G. Esteves Da Silva, *Crit. Rev. Anal. Chem.* 45 (2015) 32.
- [17] A. Seki, K. Motoya, S. Watanabe, and I. Kubo, *Anal. Chim. Acta* 382 (1999) 131.
- [18] J. Saurina, E. Lopez-Aviles, A. L. Moal, and S. Hernandez-Cassou, *Anal. Chim. Acta* 464 (2002) 89.
- [19] E. D. Malinowska, A. Manzoni, and M. E. Meyerhoff, *Anal. Chim. Acta* 382 (1999) 265.
- [20] S. Bainiwal, S. Chandra, A. Panwar, and A. K. Singh, *Talanta* 50 (1999) 499.
- [21] V. K. Gupta, R. Prasad, and A. Kumar, *Talanta* 63 (2004) 1027.
- [22] A. Malon, and M. Maj-Zurawska, *Anal. Chim. Acta* 448 (2001) 251.
- [23] M. V. Rouilly, M. Badertscher, E. Pretsch, G. Sutar, and W. Simon *Anal. Chem.* 60 (1998) 2013.
- [24] F. Lanter, D. Erne, D. Ammann, and W. Simon, *Anal. Chem.* 52 (1980) 2400.
- [25] Z. Hu, T. Buehrer, M. Mueller, B. Rusterholz, M. Rouilly, and W. Simon, *Anal. Chem.* 61 (1989) 574.
- [26] N. A. Chaniotakis, J. K. Tsagatakis, E. A. Moschou, S. J. West, and X. Wen, *Anal. Chim. Acta* 356 (1997) 105.
- [27] T. Alizadeh, and S. Azizi, *Biosens. Bioelectron.* 8 (2016) 198.
- [28] T. Alizadeh, and S. Amjadi, *J. Hazard. Mater.* 190 (2011) 451.
- [29] S. Hussain, S. Khan, S. Gul, M. I. Pividori, and M. D. P. T. Sotomayor, *React. Fun. Polym.* 106 (2016) 51.
- [30] C. Branger, W. Meouche, and A. Margaillan, *React. Fun. Polym.* 73 (2013) 859.
- [31] T. Alizadeh, M. R. Ganjali, M. Akhoundian, and P. Norouzi, *Microchim. Acta* 183 (2016) 1123.
- [32] T. Alizadeh, *Biosens. Bioelectron.* 61 (2014) 532.
- [33] T. Alizadeh, R. E. Sabzi, and H. Alizadeh, *Talanta* 147 (2016) 90.
- [34] T. Alizadeh, and M. Rashedi, *Anal. Chim. Acta* 843 (2014) 7.
- [35] A. H. Kamel, F. T. C. Moreir, S. A. A. Almeida, and M. G. F. Sales, *Electroanalysis* 20 (2008) 194.
- [36] K. P. Prathish, K. Prasad, T. P. Rao, and M. V. S. Suryanarayan, *Talanta* 71 (2007) 1976.
- [37] R. Liang, R. Zhang, and W. Qin, *Sens. Actuators B* 141 (2009) 544.
- [38] A. H. Kamel, T. Y. Sororac, and F. M. Al Romian, *Anal. Methods* 4 (2012) 3007.
- [39] T. Alizadeh, and M. Akhoundian, *Electrochim. Acta* 55 (2010) 3477.
- [40] M. Pesavento, G. D. Agostino, R. Biesuz, G. Alberti, and A. Profumo, *Electroanalysis*, 24 (2012) 813.

- [41] T. Alizadeh, M. Rashedi, Y. Hanifehpour, and S. W. Joo, *Electrochim. Acta* 178 (2015) 877.
- [42] P. Gai, Z. Guoz, F. Yang, J. Duan, T. Hao, and S. Wang, *Russ. J. Electrochem.* 47 (2011) 940.
- [43] S. Srebnik, *Chem. Mater.* 16 (2004) 883.
- [44] H. A. Zamani, F. Malekzadegan and M. R. Ganjali, *Anal Chim Acta* 555 (2006) 336.
- [45] M. R. Ganjali, P. Norouzi, F. S. Mirnaghi, S. Riahi and F. Faridbod, *IEEE Sens. J.* 7 (2007) 1138.
- [46] M. R. Ganjali, R. Kiani-Anbouhi, M. Shamsipur, T. Poursaberi, M. Salavati-Niasari, Z. Talebpour and M. Emami, *Electroanalysis* 16 (2004) 1002.
- [47] M. R. Ganjali, S. Rasoolipour, M. Rezapour, P. Norouzi, A. Tajarodi and Y. Hanifehpour, *Electroanalysis* 17 (2005) 1534.
- [48] F. Faridbod, M. R. Ganjali, B. Larijani, P. Norouzi, S. Riahi and F. S. Mirnaghi, *Sensors* 7 (2007) 3119.
- [49] M. R. Ganjali, A. Roubollahi, A. R. Mardan, M. Hamzeloo, A. Mogimi and M. Shamsipur, *Microchem. J.* 60 (1998), 122.
- [50] T. Alizadeh, M. R. Ganjali and M. Zare, *Anal. Chim. Acta* 689 (2011) 52.
- [51] H. A. Zamani, M. Nekoei, M. Mohammadhosseini and M. R. Ganjali, *Mater. Sci. Eng. C* 30 (2010) 480.